

HETEROGENEOUS DETONATIONS

S. M. Frolov

N. N. Semenov Institute of Chemical Physics
Russian Academy of Sciences
Moscow, Russia

The paper provides a rational theory of heterogeneous detonation including finite-rate multistep ignition and combustion chemistry as well as group-screening effects of drops in suspensions. The theory is capable of predicting the effects of mixture equivalence ratio, drop size, fuel type, active additives, fuel prevaporization degree, initial pressure and temperature, etc. on detonation structure and limits. Possible mechanisms of detonation propagation are discussed.

Introduction

Air-breathing propulsion systems operating on propagating periodic detonations have recently become a topic of intense research and development [1]. One of the most challenging problems relevant to such propulsion systems is to provide the conditions and techniques to repeatedly initiate heterogeneous detonation waves at short distances with very low external energy deposition. Also, heterogeneous detonations are known to be a cause of devastating effects at uncontrolled accidental explosions in industry.

Contrary to detonations in premixed gases, chemical energy deposition in a heterogeneous detonation wave is preceded by mixture formation. Despite the difference in the mechanism of energy release, thermodynamically gaseous and heterogeneous detonations are very similar to each other. At similar initial conditions, they have almost same propagation velocities. Moreover, both propagate due to strong coupling between the lead shock wave and chemical energy deposition. In suspensions of very fine hydrocarbon drops in oxygen, the observed structure of a heterogeneous detonation wave resembles the structure of the corresponding gaseous detonation. The necessity of ensuring

the stability of the “shock wave–reaction zone” complex implies that the reaction completion time in gaseous and heterogeneous detonations should not differ considerably.

The current understanding of heterogeneous detonations is based more on general similarity with gaseous detonations rather than on the rational quantitative theory. The existing theoretical models of the heterogeneous detonation consider the average flow behind the lead shock wave [2–7]. Interactions between drops and gas are most often described using various (mostly irrelevant) empirical correlations obtained for a single spherical particle in the steady-state gas flow. Such models do not account for finite rates of chemical reactions and fail to predict detonability limits. In some cases, either empirical correlations for ignition delays or detailed fuel oxidation mechanisms are applied to describe the detonation structure based on the averaged temperature and gas-phase composition, thus ignoring high intrinsic sensitivity of chemical transformations to local mixture temperature and composition. Finally, in all available models, the screening effects of neighbor drops on interphase mass, momentum, and energy fluxes are modeled indirectly, through instantaneously-changing averaged values of gas flow parameters. As a result, the finite rates of accompanying physical and chemical phenomena are completely neglected.

The objective of this paper is to develop a quantitative theory of heterogeneous detonations which could allow revealing possible mechanisms of detonation propagation, as well as predicting the detonation structure, propagation velocity, and detonability limits depending on physical and chemical properties of liquid fuel as well as initial conditions.

Phenomenology

Detonation is the steady-state self-sustained supersonic combustion mode propagating due to shock-induced chemical energy release. To get an idea about the mean values of thermodynamic parameters and flow velocity in the detonation wave, one can assume that the heterogeneous detonation exhibits the classical one-dimensional (1D) Zel’dovich–von Neumann–Doering (ZND) structure very similar to the 1D structure of gaseous detonation. In the frame of reference moving with the

detonation wave, the lead front is the inert shock wave propagating at supersonic velocity D . The lead front is followed by the subsonic reaction zone with energy deposition to the postshock flow due to gas-phase chemical reactions between fuel, oxidizer, and various intermediate reaction products. The subsonic reaction zone is terminated by the Chapman–Jouguet (CJ) plane where the gas velocity attains the local speed of sound, thus avoiding penetration of weak gasdynamic disturbances upstream.

In the adopted frame of reference, the two-phase medium consisting of liquid fuel drops and air approaches the shock wave with temperatures T_{d0} and T_{g0} , respectively, at constant velocity D equal to the detonation velocity. Due to high dynamic and thermal inertia of liquid drops as compared to gas, the drops enter the reaction zone with velocity $u_{ds} = D$ and initial temperature $T_{ds} = T_{d0}$ whereas the gas “instantaneously” changes its velocity in the shock wave from D to u_{gs} and temperature from T_{g0} to T_{gs} . This is the reason why various physical and chemical processes are activated immediately behind the lead shock wave, namely, drop deceleration, deformation and aerodynamic breakup, drop-mist dispersion, heating, vaporization, mixing of fuel vapor with oxidizer, ignition, and combustion. Since these processes are highly interrelated with each other, the entire phenomenon of heterogeneous detonation looks very complex even in the 1D formulation.

The typical values of main characteristic parameters for the detonation of a stoichiometric hydrocarbon–air mixture at normal initial conditions (air pressure $p_0 = 1$ bar, density $\rho_{g0} = 1.2$ kg/m³, temperature $T_{g0} = 293$ K, and the speed of sound $a_{g0} = 340$ m/s) are listed in Table 1. These are the detonation velocity D , detonation Mach number $M = D/a_{g0}$, gas pressure p_s , density ρ_{gs} , temperature T_{gs} , and velocity u_{gs} immediately behind the lead shock wave, and gas pressure p_{CJ} , density ρ_{CJ} , temperature T_{CJ} , and velocity u_{CJ} in the CJ plane. It follows from Table 1 that immediately behind the lead shock wave the differences in phase velocities $\Delta u = u_{ds} - u_{gs} = D - u_{gs}$ and temperatures $\Delta T = T_{gs} - T_{ds} = T_{gs} - T_{d0}$ attain very high values: approximately 1500 m/s and 1400 K, respectively. As mentioned above, these differences become driving forces for intense interphase fluxes of mass, momentum, and energy.

When studying the heterogeneous detonation, one usually deals with initially nonuniform polydispersed drop suspensions. Drop sus-

Table 1 Main characteristic parameters of hydrocarbon fuel–air heterogeneous detonation

D ,	M	p_s ,	ρ_{gs} ,	T_{gs} ,	u_{gs} ,	p_{CJ} ,	ρ_{CJ} ,	T_{CJ} ,	u_{CJ} ,
m/s		bar	kg/m ³	K	m/s	bar	kg/m ³	K	m/s
1800	5.3	35	7.2	1680	300	18	2.2	2800	980

pensions are characterized with the local liquid density η_d , drop number density n_d , and drop size distribution function. By definition, the local liquid density is given by derivative $\eta_d = dm_l/dV$ where m_l is the mass of dispersed liquid and V is the volume. Reactive sprays and drop suspensions are more frequently characterized by the local instantaneous equivalence ratio Φ defined as

$$\Phi = \frac{\eta_d}{\phi_{st}\rho_g}$$

where ρ_g is the local instantaneous gas density and ϕ_{st} is the stoichiometric fuel–air ratio.

At known η_d and n_d , one can readily determine the local instantaneous mass-mean drop radius r_d :

$$r_d = \left(\frac{3}{4\pi n_d} \right)^{1/3} \left(\frac{\eta_d}{\rho_d} \right)^{1/3}$$

where ρ_d is the drop material density. The first term in the last equation is nothing else as the local instantaneous mean radius of a spherical gas volume attributed to each droplet in suspension:

$$R = r_d \left(\frac{\rho_d}{\eta_d} \right)^{1/3}$$

For liquid hydrocarbon fuels, $\rho_d = 700\text{--}800 \text{ kg/m}^3$. Therefore, for locally stoichiometric mixtures ($\Phi = 1$ and $\phi_{st} \approx 0.06$) immediately behind the lead shock wave, where $\rho_g = \rho_{gs} \approx 7.2 \text{ kg/m}^3$ (see Table 1), the mean radius of the gas sphere attributed to each drop is about $R \approx 12r_d$. Taking into account that shock-induced breakup of drops

results in the formation of dense micromist clouds with local instantaneous equivalence ratios $\Phi \gg 1$, one comes to a conclusion that the rational theory of heterogeneous detonations must include “screening” effects of neighbor drops on the interphase mass, momentum, and energy exchange. To model the screening effects, the approach suggested in [8] will be used.

For constructing a theory it is worth first to estimate the characteristic times of the various physical and chemical processes in the detonation wave. Such estimates are presented in Table 2 for the conditions immediately behind the lead shock wave of the heterogeneous detonation (see Table 1) for single drops of different initial radius r_d . The characteristic times entering Table 2 are: τ_u for drop deceleration; τ_b for drop breakup; τ_v for drop vaporization; τ_i for drop autoignition; and τ_c for drop burning.

The characteristic time of drop deceleration was estimated as

$$\tau_u \approx \frac{8}{3} \frac{\rho_d}{\rho_g} \frac{r_d}{C_D |u_g - u_d|}$$

where C_D is the aerodynamic drag coefficient of a liquid drop. The estimates of τ_u in Table 2 are made assuming that $C_D = 0.44$ [9] and $\rho_d = 800 \text{ kg/m}^3$.

The characteristic drop breakup time τ_b was estimated as [9]:

$$\tau_b = 10 \frac{r_d}{|u_d - u_g|} \left(\frac{\rho_d}{\rho_g} \right)^{1/2}.$$

For relatively small drops with $r_d < 50 \text{ }\mu\text{m}$, time τ_b is seen to be less than 3–4 μs . This means that such drops experience aerodynamic deformation and breakup nearly immediately behind the lead shock wave producing the micromist of secondary droplets. The mean radius of micromist droplets r_m is about $r_m \sim 0.1r_{d0}$ [9].

The characteristic vaporization time τ_v of a single spherical micromist droplet in the wake of a disintegrated parent drop was estimated based on the well-known d^2 -law:

$$\tau_v \approx \frac{4r_m^2}{K}$$

where K is the vaporization constant depending on temperature and pressure. A similar d^2 -law is applicable to drop combustion, and the

Table 2 Estimated values of various characteristic times behind the detonation front

$r_d, \mu\text{m}$	$\tau_u, \mu\text{s}$	$\tau_b, \mu\text{s}$	$\tau_v, \mu\text{s}$	$\tau_i, \mu\text{s}$	$\tau_c, \mu\text{s}$
2.5	1.1		> 36		
5	2.2		> 143	3	> 50
10	4.5	< 0.7	> 570		
25	11.2	< 1.7	> 3570		
50	22.5	< 3.5			
100		< 7.0			
250		< 17.5			

corresponding constant is referred to as the combustion constant. As a matter of fact, the combustion constant is close to the vaporization constant under conditions when the ambient gas temperature is equal to the fuel combustion temperature. At atmospheric pressure, the combustion constant for relatively large *n*-heptane drops ($r_d > 50 \mu\text{m}$) is $K \approx 0.7 \text{ mm}^2/\text{s}$ [10]. Both vaporization and combustion constants are known to decrease with pressure [11]. Thus, to obtain a conservative estimate for τ_v at conditions behind the lead shock wave, the value of $K \approx 0.7 \text{ mm}^2/\text{s}$ was used. The estimated values of τ_v in Table 2 are somewhat smaller than the values obtained by detailed calculations of drop vaporization based on the approach reported in [12]. Note that drop vaporization time in dense drop suspensions increases with Φ , i. e., the estimate of τ_v shown in Table 2 is well conservative.

The characteristic time of micromist drop autoignition τ_i (ignition delay) was calculated using the approach reported in [12]. The localized autoignition of fuel vapor occurs at a certain distance from the drop surface. At the ignition location, the fuel vapor and oxygen concentrations are considerably lower than at the drop surface and at a large distance from the drop, respectively. Time τ_i was defined as the time taken for the maximum rate of local temperature rise to attain a preset value of 10^7 K/s . The calculations for the micromist drop with $r_m = 5 \mu\text{m}$ indicate (see Table 2) that $\tau_i \approx 3 \mu\text{s}$ and does not depend on Φ within a wide range: from $\Phi = 0.0012$ to 12.

The characteristic burning time τ_c presented in Table 2 was calculated for a micromist drop with $r_m = 5 \mu\text{m}$ based on approach [12].

Similar to vaporization, combustion in dense drop suspensions is sensitive to local instantaneous equivalence ratio Φ . The lifetime of burning drops increases with Φ .

As is seen from Table 2, the characteristic times relate to each other as: $\tau_v \sim \tau_c$, $\tau_v, \tau_c \gg \tau_i$, $\tau_v \cdot \tau_c \gg \tau_b$, $\tau_v, \tau_c \gg \tau_u$, and $\tau_u > \tau_b$.

Model

The above estimates of the characteristic times of various physical and chemical phenomena inherent in the heterogeneous detonations indicate that the energy release in the detonation wave is mostly affected by the duration of combustion of micromist droplets in the wake of disintegrated parent drops. Keeping in mind that according to Table 2 the drops of initial radius $r_d \sim 100 \mu\text{m}$ and smaller disintegrate completely during the characteristic time τ_b less than $7 \mu\text{s}$ and the micromist droplets of radius $r_m \sim 0.1r_d$ exhibit the characteristic deceleration time τ_u less than $5 \mu\text{s}$ (see Table 2), one can neglect (in the first approximation) the durations of parent drop breakup and micromist drop deceleration processes. In this approximation, the lead shock wave “instantaneously” converts the drops of radius r_d to micromist drops of radius $r_m \sim 0.1r_d$. Moreover, the micromist drops “instantaneously” decelerate to the gas velocity u_{gs} . In view of it, the difference in phase temperatures, $\Delta T = T_{gs} - T_{ds} = T_{gs} - T_{d0}$, can be considered as the only driving force determining the interphase mass and energy exchange in the heterogeneous detonation wave. Furthermore, since the relationship $r_m \sim 0.1r_d$ provides only a rough estimate for the micromist drop radius, there is apparently a sense to study the heterogeneous detonations of monodisperse rather than polydisperse drop suspensions. Despite this approximation does not take into account possible initial effects caused by convective heat and mass transfer between phases as well as secondary breakup of micromist drops and their size distribution, it takes into account an intrinsically important feature of heterogeneous detonation that is the localized two-phase mixture ignition and combustion under conditions of micromist cloud.

Thus, the model of heterogeneous detonation can be reduced to considering a stationary 1D detonation wave propagating in a uniform monodispersed suspension of hydrocarbon fuel drops in air at initial

pressure p_0 and initial temperatures of phases $T_{g0} = T_{d0}$ or $T_{g0} \neq T_{d0}$. It implies that the gas and monodisperse drops of initial radius r_d approach the lead shock wave at velocity D . When the gas crosses the shock front, its velocity u_g , density ρ_g , pressure p , and temperature T_g exhibit jump-wise changes to u_{gs} , ρ_{gs} , p_s , and T_{gs} . As for the drops, upon crossing the lead shock front, they instantaneously experience aerodynamic breakup to micromist drops of radius $r_m = 0.1r_d$ and the velocity of the micromist drops decreases instantaneously to the gas velocity: $u_{ds} = u_{gs}$. The other parameters of micromist drops immediately behind the lead shock wave (liquid density ρ_{ds} and temperature T_{ds}) remain equal to those of the parent drops ahead of the detonation wave.

Within the adopted approximation, the problem on micromist drop ignition and combustion in the postshock two-phase flow can be considered assuming spherical symmetry of all physical and chemical processes in the vicinity of fuel drops. The gas flow behind the lead shock wave can be described by the mean values of $u_g(x)$, $\rho_g(x)$, $p(x)$, and $T_g(x)$ where x is the streamwise distance from the lead shock front. Due to the fact that immediately behind the lead shock there is a large difference between gas and drop temperatures, fuel drops start evaporating. At certain conditions, the fuel vapor–air mixture in the drop vicinity exhibits autoignition and the drops start burning. As a result, the mean flow parameters u_g , ρ_g , p , and T_g get changing with distance x or time t (distance and time are related to each other as $dx = u_g dt$). The mean composition of the gas flow (mean molecular mass W_g) changes as well.

The steady-state 1D structure of the heterogeneous detonation is thus governed by the set of equations including the differential conservation equations of mass, momentum, and energy for the mean postshock flow (mean flow model) coupled with the detailed model of liquid fuel drop vaporization, ignition, and combustion (drop model). The drop model is based on the conjugate set of nonstationary partial differential equations of heat and mass transfer between liquid and gas phases with multicomponent diffusion and multistage chemical reaction taken into account. The screening effects of neighbor drops in suspension are introduced via proper boundary conditions at the outer boundary of the gas sphere surrounding an individual drop [8, 12]. Thus, the statement of the problem allows for the continuous monitoring of local chemical and physical processes in the interdrop space simultaneously

with monitoring the variation of mean flow parameters behind the lead shock wave. The existence condition for the heterogeneous detonation is based on the generalized CJ conditions derived from the governing equations. The solution of the problem provides detonability limits as functions of all governing parameters. As a reference liquid fuel, *n*-heptane is considered with the multistage oxidation mechanism taken from [13]. Note that such a theory does not contain any empirical or “tuning” parameter.

A set of governing equations is integrated numerically with the use of the nonconservative implicit finite-difference scheme and movable adapted computational grid. The solution procedure includes iterations at each time step. The accuracy of the solution is controlled by checking the elementary balances of C and H atoms as well as the energy balance at each time step.

Results

Figure 1 shows the predicted time histories of temperature (*a*) and species mass fractions (*b*) in the heterogeneous detonation wave propagating in the monodisperse *n*-heptane suspension with the initial drop radius $50\ \mu\text{m}$, at initial pressure 1 bar, initial gas temperature 293 K, initial liquid temperature 293 K, and $\Phi \approx 2.5$ ($\eta_d = 0.2\ \text{kg/m}^3$). According to the adopted assumption, the micromist drops formed immediately behind the lead shock wave have radius $r_m = 0.1r_d = 5\ \mu\text{m}$. The convergent solution in these conditions corresponds to $D = 1824\ \text{m/s}$.

The following specific features of the heterogeneous detonation structure evident from Fig. 1 are worth to be mentioned:

- there is the induction period behind the lead shock wave. For the case under consideration, the duration of the induction period is about $3\ \mu\text{s}$ (see Fig. 1*a*);
- during the induction period, the mean gas temperature decreases (see Fig. 1*a*); mass fraction of fuel vapor increases nearly linearly with time, whereas the mass fraction of oxygen slightly decreases (see Fig. 1*b*);
- ignition occurs when the mean mass fraction of fuel vapor in the postshock flow attains the value of about 0.003 and the mean

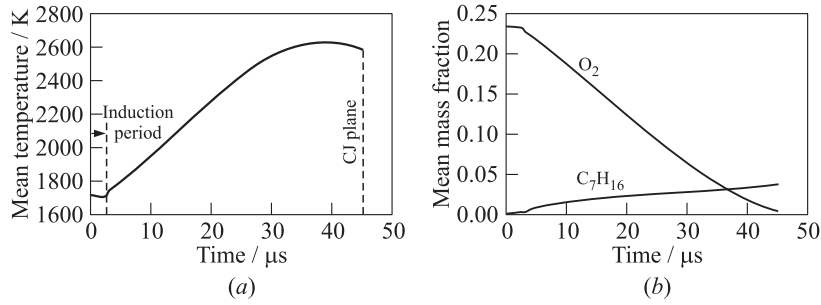


Figure 1 Predicted evolution of temperature (a) and mass fractions of *n*-heptane and oxygen (b) in the heterogeneous detonation wave propagating in the monodisperse *n*-heptane suspensions with the initial drop radius of 50 μm (micromist drop radius of 5 μm) at 1 bar, 293 K, and $\Phi \approx 2.5$ ($\eta_d = 0.2 \text{ kg/m}^3$)

oxygen mass fraction is about 0.23. As the molecular mass of *n*-heptane is 100 kg/kmol, this implies that the mean fuel-to-oxygen mass ratio at ignition is equal to $(0.003 \cdot 100)/(0.23 \cdot 32) = 0.04$. Remind that the stoichiometric fuel-to-oxygen molar ratio in the premixed *n*-heptane–air mixture is $1/11 = 0.091$ which gives the fuel-to-oxygen mass ratio as $100/(11 \cdot 32) = 0.284$. This means that ignition occurs in the vapor phase when the mean mixture composition in the postshock flow is very fuel lean. This effect was not ever taken into account in the earlier models;

- ignition results in the fast rise of mean temperature from about 1700 to 1740 K, oxygen mass fraction decrease from 0.23 to 0.227, and fuel mass fraction decrease from 0.003 to 0.0022. This (fast) ignition stage corresponds to burnout of only small amount of the nonuniform premixed fuel–air mixture around fuel drops. Further energy release occurs in the diffusion controlled mode, i. e., the rate of energy release is controlled by drop vaporization and fuel vapor diffusion toward the flame. The latter follows from the change in the slope of temperature in Fig. 1a and mass fractions of fuel and oxygen in Fig. 1b. The slope of the fuel mass fraction curve at this stage of the process becomes nearly the same

- as in the induction zone, when fuel vapor accumulation rate was controlled by liquid vaporization. Note that the early models assumed that the ignition stage consumed all accumulated vapor rather than its small portion;
- the combustion constant at the diffusion-controlled stage is about 0.8–0.9 mm²/s which is close to the value of 0.7 mm²/s measured experimentally for relatively large *n*-heptane drops (50–70 μm in diameter) at normal initial conditions [10]. The arising difference in the combustion constants is explained by the effects of elevated temperature and pressure in the detonation wave;
 - prior to the CJ plane, the temperature in the reaction zone of the heterogeneous detonation goes through the maximum, which is consistent with the ZND detonation structure; and
 - the total duration of the reaction zone in Fig. 1 is about 45 μs, including the induction period (~ 3 μs). Thus, the duration of the energy release zone (~ 42 μs) is an order of magnitude longer than the induction period. Note that in the early models, the reaction zone duration was often assumed equal to the induction period.

Figure 2 shows the predicted time histories of temperature (*a*) and oxygen mass fraction (*b*) around an individual drop in the micromist for the conditions relevant to Fig. 1. One can see that

- ignition occurs locally with the delay ~ 3 μs behind the shock wave at a distance of about two drop radii from the drop center (see Fig. 2*a*). At the ignition instant, there is a considerable amount of fuel vapor accumulated near the drop. Ignition is accompanied with the localized depletion of oxygen (see Fig. 2*b*) and production of combustion products (mainly CO₂, CO, and H₂);
- the temperature in the arising flame quickly attains the value of about 2800–2900 K which is considerably higher than the mean temperature in Fig. 1*a* at the corresponding time instants (3–10 μs). The flame propagates outward from the drop surface at the apparent velocity of about 1.5 m/s. At the end of reaction, the flame decelerates to about 0.9 m/s. Note that the early models

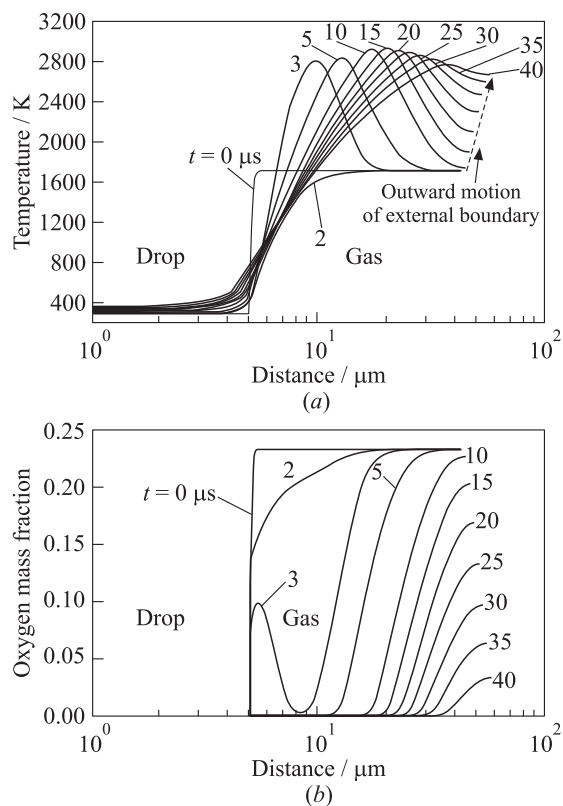


Figure 2 Predicted time histories of temperature (a) and oxygen mass fraction (b) around an *n*-heptane drop in the micromist for the conditions relevant to Fig. 1. Numbers correspond to different time instants (in microseconds) counted from shock compression ($t = 0$). Ignition occurs at approximately $3 \mu\text{s}$

operated primarily with the mean temperature disregarding huge temperature and density gradients in the space between drops;

- contrary to the single-drop flame in the unconfined oxidizing atmosphere, the flame in the fuel-rich drop suspension moves outward until nearly all available oxygen is depleted (see Fig. 2b);

- at the end of reaction ($\sim 45 \mu\text{s}$) the space around the drop contains some amount of intermediate products (CO and H_2) and much unreacted fuel vapor mixed with hot combustion products. In the reaction zone, the drop radius decreased from 5 to about $3.8 \mu\text{m}$. Note that the early models did not consider the accumulation of fuel vapor and intermediate products in the space between drops filled with hot combustion products;
- expansion process caused by exothermal chemical reactions results in the expansion of the gas sphere around the drop as is evident from the outward motion of sphere radius R in Fig. 2; and
- temperature distribution inside the drop is nonuniform when it leaves the reaction zone through the CJ plane (refer to time instant $40 \mu\text{s}$ in Fig. 2*a*). The temperature of the drop surface quickly attains the saturation temperature on the level of 490–500 K so that the difference between liquid temperatures at the drop surface and in the drop center attains 150–190 K. The fact that the heated drops leave the reaction zone should obviously be treated as the heat loss.

Figure 3 shows the predicted time histories of temperature (*a*) and fuel mass fraction (*b*) in self-sustained detonation waves propagating in monodisperse *n*-heptane drop suspensions with the initial drop radius $r_d = 50 \mu\text{m}$ ($r_m = 0.1r_d = 5 \mu\text{m}$) at different equivalence ratios Φ , at initial pressure 1 bar, initial gas temperature 293 K, and initial liquid temperature 293 K. When analyzing the results of calculations partly presented in Fig. 3 one comes to the following important general observation.

The reaction zone of the heterogeneous detonation consists of three characteristic periods, namely, (*i*) induction period (the time interval between shock compression of the two-phase mixture and fuel vapor autoignition); (*ii*) period of fast volumetric autoignition and combustion of some finite mass of accumulated fuel vapor; and (*iii*) period of diffusion-controlled frontal combustion of fuel drops. At low equivalence ratios ($\Phi = 0.75, 1.0, \text{ and } 2.5$), the energy release in the heterogeneous detonation is governed by the frontal diffusion-controlled combustion (third period) which results in relatively long reaction zones ($50\text{--}120 \mu\text{s}$ in Fig. 3). At large equivalence ratios ($\Phi = 15 \text{ and } 30$), the energy release is governed by the volumetric autoignition and combustion of

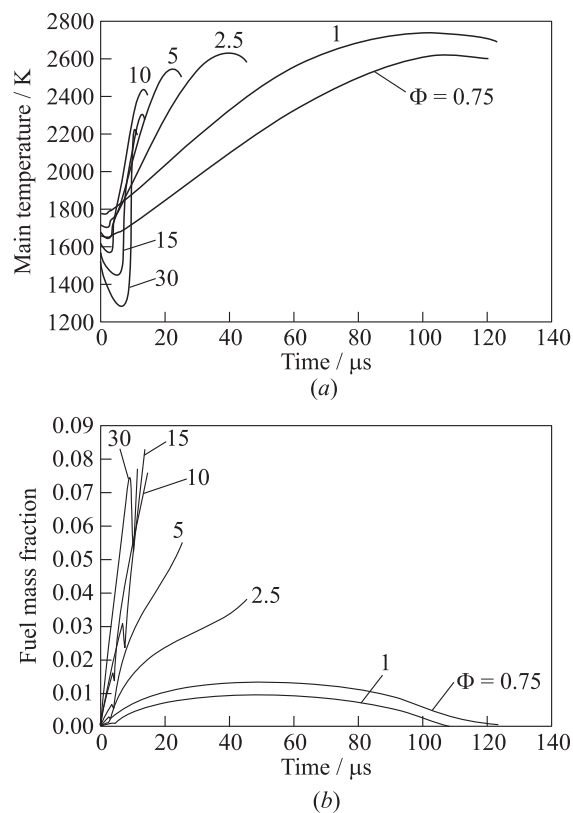


Figure 3 Time histories of temperature (a) and fuel mass fraction (b) in self-sustained detonation waves propagating in monodisperse *n*-heptane suspensions with the initial drop radius $50 \mu\text{m}$ (micromist drop radius $5 \mu\text{m}$) at different equivalence ratios. Initial pressure is 1 bar, initial gas temperature is 293 K, initial liquid temperature is 293 K

some amount of accumulated fuel vapor (second period) which leads to relatively short reaction zones ($\sim 10 \mu\text{s}$ in Fig. 3). At intermediate equivalence ratios ($\Phi = 5$ and 10), the energy release is governed by a combined (frontal and volumetric) mechanism with the comparable contributions of both modes to the total reaction time. By other words,

the mechanism of energy release in the heterogeneous detonations depends on the suspension density: increase in the suspension density results in the transition from the diffusion controlled to the kinetically controlled mode of energy deposition. The other important result relates to the existence of fuel-lean and fuel-rich detonability limits for the heterogeneous detonations (for the conditions of Fig. 3, $\Phi \approx 0.75$ and 35, respectively). The fuel-rich detonability limit is considerably wider than that for the premixed compositions whereas the fuel-lean limit is close to that in the premixed composition.

In addition to the general results outlined above, Fig. 3 provides the following particular findings:

- the reaction time is maximum ($\sim 123 \mu\text{s}$) for the stoichiometric mixture ($\Phi = 1$) and decreases toward the detonability limits. At the fuel-lean detonability limit, it is about $120 \mu\text{s}$, whereas at the fuel-rich detonability limit, it is about $11 \mu\text{s}$;
- the maximum temperature in the reaction zone decreases considerably with the equivalence ratio. For the stoichiometric mixture ($\Phi = 1$), it is about 2750 K whereas at the fuel-lean and fuel-rich limits it is about 2620 and 2200 K, respectively;
- contrary to the reaction time, the induction period is minimal for the stoichiometric mixture ($\tau_i \approx 2 \mu\text{s}$) and increases toward the detonability limits. At the fuel-lean limit, the induction period is much smaller than the reaction time ($\tau_i \approx 3 \mu\text{s}$), while at the fuel-rich limit these times are nearly equal to each other ($\tau_i \approx 10 \mu\text{s}$);
- the largest decrease in the mean gas temperature during the induction period is attained at the fuel-rich limit (about 240 K), as is evident from Fig. 3a;
- at the fuel-lean limit, reaction proceeds mostly in the diffusion controlled mode, while at the rich limit, it proceeds in the kinetically controlled mode (detonation is supported by the abrupt explosion-like autoignition of the prevaporized fuel mixed with air); and
- in the stoichiometric mixture, fuel and oxygen react almost completely. Contrary to the stoichiometric mixture, at the fuel-lean

limit, there exists some unburned fuel in the CJ plane (0.05%(wt.)), while at the fuel-rich limit there is some unburned oxygen in the CJ plane (about 2.3%(wt.)). The incomplete combustion of oxygen in fuel-rich suspensions is mainly caused by considerable thermal losses from the reaction zone with the nonevaporated drops crossing the CJ plane.

Concluding Remarks

A rational theory of heterogeneous detonations containing no empirical fitting or “tuning” parameter has been developed. The capabilities of the theory are discussed based on the computational results for *n*-heptane–air detonations at different equivalence ratios.

The reaction zone of the heterogeneous detonation was found to consist of three characteristic periods, namely, (*i*) induction period; (*ii*) period of fast volumetric autoignition and combustion of some finite mass of accumulated fuel vapor; and (*iii*) period of diffusion-controlled frontal combustion of fuel drops. At low equivalence ratios on the order of 1.0, the energy release in the heterogeneous detonation is governed by the frontal diffusion-controlled combustion, which results in relatively long reaction zones and high sensitivity of the detonation velocity and reaction zone structure to the equivalence ratio and drop size. At very large equivalence ratios closer to the fuel-rich detonability limit, the energy release is governed by the fast volumetric autoignition and combustion of some amount of accumulated fuel vapor, which leads to very short reaction zones and low sensitivity of the detonation velocity and reaction zone structure to the equivalence ratio and drop size. At intermediate equivalence ratios, the energy release is governed by a combined frontal and volumetric mechanism with the comparable contributions of both modes to the total reaction time. By other words, the mechanism of energy release in the heterogeneous detonations depends on the suspension density: increase in the suspension density results in the transition from diffusion controlled to the kinetically controlled mode of energy deposition.

Due to the resolution of local physical and chemical phenomena, including finite-rate multistep ignition and combustion chemistry and group-screening effects of drops in suspensions, the present theory is

capable of predicting the influence of fuel type, active additives, pressure, gas and liquid temperature, as well as the liquid prevaporization degree on the detonability limits and detonation structure. Also, it is capable of treating the effects produced by confinement in terms of heat and momentum losses at rigid walls. These effects will be studied in the future.

Among the unresolved issues lacking in the 1D steady-state theory under consideration, one has to mention various transient and multidimensional phenomena inherent in realistic heterogeneous detonations. First of all, these are the issues dealing with simulating the intrinsically unsteady (pulsating) mode of detonation propagation observed experimentally. The heterogeneous detonations are known to exhibit localized explosions in the reaction zone giving rise to a complex multidimensional wave structure resembling the irregular cellular structure of gaseous detonations. The other important unresolved issue is the detonation response to various disturbances like spatial nonuniformity of drop suspension density, drop size distribution, fuel vapor concentration, etc. The last but not least is the issue of detonation initiation.

Acknowledgments

Valuable contribution of V. Ya. Basevich, A. A. Belyaev, V. S. Posvyanskii, and V. A. Smetanyuk to the studies reviewed in this paper are gratefully acknowledged. This work was supported by the Russian Foundation for Basic Research (grant 08-08-00068) and Federal program "Scientific and teaching human resources of innovative Russia" for 2009–2013.

References

1. Roy, G. D., S. M. Frolov, A. A. Borisov, and D. W. Netzer. 2004. Pulse detonation propulsion: Challenges, current status, and future perspective. *Progr. Energy Combust. Sci.* 30(6):545–672.
2. Borisov, A. A., B. E. Gelfand, S. A. Gubin, S. M. Kogarko, and A. L. Podgrebenkov. 1970. The reaction zone of two-phase detonations. *Astronautica Acta* 15:411–19.

3. Zhdan, S. A. 1977. Calculation of heterogeneous detonation with regard for fuel drop deformation and breakup. *Combust. Explosion Shock Waves* 13(2):258–62.
4. Gubin, S. A., and M. Sichel. 1977. Calculation of the detonation velocity of liquid droplets and gaseous oxidizer. *Combust. Sci. Technol.* 17(3–4):109–17.
5. Eidelman, S., and A. Burkat. 1980. Evolution of a detonation wave in a cloud of fuel droplets. Part I: Influence of ignition explosion. *AIAA J.* 18(9):1103–9.
6. Voronin, D. V., and S. A. Zhdan. 1984. Calculation of initiation of the heterogeneous detonation in tube by the explosion of hydrogen–oxygen mixture. *Combust. Explosion Shock Waves* 20(4):112–16.
7. Sichel, M. 1991. Numerical modeling of heterogeneous detonations. In: *Numerical approaches to combustion modeling*. Eds. E. S. Oran and J. P. Boris. Progress in astronautics and aeronautics science ser. New York: AIAA Inc. 135:447–58.
8. Frolov, S. M., V. Ya. Basevich, V. S. Posvianskii, and V. A. Smetanyuk. 2004. Vaporization and combustion of a hydrocarbon fuel drop. Part IV: Drop vaporization with regard for spray effects. *Russ. J. Chem. Phys.* 23(7):49–58.
9. Nigamtulin, R. I. 1987. *Dynamics of multiphase media*. Vol. 1. Moscow: Nauka Publ.
10. Frolov, S. M., V. Ya. Basevich, A. A. Belyaev, V. S. Posvyanskii, and V. A. Smetanyuk. 2005. Modeling of drop evaporation and combustion with regard for spray effects. In: *Combustion and pollution: Environmental effect*. Eds. G. D. Roy, S. M. Frolov, and A. M. Starik. Moscow: TORUS PRESS. 117–32.
11. Frolov, S. M., V. S. Posvyanskii, V. Ya. Basevich, A. A. Belyaev, V. A. Smetanyuk, V. V. Markov, and I. V. Semenov. 2004. Vaporization and combustion of hydrocarbon fuel drop. Part II: Nonempirical model of drop vaporization with regard for multicomponent diffusion. *Russ. J. Chem. Phys.* 23(4):75–83.
12. Frolov, S. M., V. Ya. Basevich, F. S. Frolov, A. A. Borisov, V. A. Smetanyuk, K. A. Avdeev, and A. N. Gots. 2009. Correlation between drop vaporization and self-ignition. *Russ. J. Phys. Chem. B* 3:333–47.
13. Frolov, S. M., V. Ya. Basevich, M. G. Neuhaus, and R. Tatshl. 1997. In: *Advanced computation and analysis of combustion*. Eds. G. D. Roy, S. M. Frolov, and P. Givi. Moscow: ENAS Publ. 537.